

Magnetic properties of spin- $\frac{7}{2}$ Blume-Capel chain under a magnetic field

M. Karimou^{a,b,*}, M. Bati^c

^a Ecole Nationale Supérieure de Génie Énergétique et Procédés (ENSGEP) d'Abomey, Benin

^b Institut de Mathématiques et de Sciences Physiques (IMSP), Benin

^c Recep Tayyip Erdoğan University, Department of Physics, Rize, Turkey

ARTICLE INFO

Communicated by Rappoport Tatiana.

Keywords:

Blume-Capel model
Transfer matrix method
Magnetization plateaus
Spin- $\frac{7}{2}$
Ising chain

ABSTRACT

A magnetic property of the one dimensional spin- $\frac{7}{2}$ Blume-Capel model under the magnetic field has been investigated by means of transfer matrix method. Thermodynamic response functions are also obtained for varying values of reduced thermodynamic temperature and scaling magnetic field. We have seen that the crystal field strongly affects magnetic plateau mechanism. Our simulation results demonstrate that the plateau becomes smoother when the value of the temperature increased. Entropy of the system goes to zero rapidly for positive crystal field values so we see only saturation values of the system. We observed that the minimum of specific heat tends to shift to the relatively lower thermodynamic temperature regions as the strength of the crystal field is increased.

1. Introduction

In the past decades, there has been a great deal of interest in the study of Ising spins systems due to their theoretical interest and possible technological applications such as storage devices, permanent magnets, sensors, etc [1–3].

In particular, the magnetic properties of low spin Ising systems have been intensively studied both theoretically and experimentally. Some works in the field could be mentioned. On the theoretical side, the previous studies are mainly devoted to one dimensional (1D) systems with small spins ($S = 1/2$ or 1) to study the magnetic properties of the one-dimensional (chain) structures [4–11]. The behavior of the spin-correlation function in one-dimensional spin- $1/2$ Ising chains has been theoretically studied [8]. The exact solution of the 1D Ising models has been obtained for spin- S Ising chains [12,13] under an external magnetic field.

The investigations were expanded to higher spin values. Such as Gambardella was reported that a ferromagnetic (FM) ordering could be observed in a single Co magnetic atom or finite size of 1D atomic chain (Higher spin ($S = 3/2$) Co(II)) [14,15]. Beside the strictly linear structures both inorganic [16] and organic [17] compounds displaying the quasi 1D structures [18]. In experimental studies the higher-order spin couplings have been observed in some magnetic compound such as MnO and NiO [19,20]. Asha et al. is synthesized three different compounds. Each of these compounds consists of weakly interacting chains of Mn²⁺

with $S = 5/2$, and magnetically behave as one-dimensional antiferromagnetic $S = 5/2$ chains [21,22]. Other systematic studies on chain-based spin systems were carried out on [(CH₃)₄N]MnCl₃ [23–25], CsMnCl₃·2H₂O [26], and CsMnBr₃ [27]. They introduced that antiferromagnetic interaction represented by $S = 5/2$. The magnetic responses of Gd³⁺ and Yb³⁺ are well described by $S = 7/2$ spin systems [28].

One of the important issue on this matter is the effect of the crystal field interaction on the magnetic response, which has been investigated by Blume-Capel (BC) model. The various theoretical model and method for issue can be found in Refs. [29]. So far their intrinsic mechanisms of magnetic exchange interactions are still a puzzle. Systematic experiments on high-quality single crystals or stoichiometric samples are necessary. Theoretical and numerical tools often considered in such investigations are: Transfer Matrix Method (TMM) [8,29–32], Mean-Field Approximation [33–41] Effective Field Theory [42,43], Green's function formalism [44], Bethe lattice treatment [45–47] Monte Carlo Simulation [48,49] etc. The thermodynamic properties of one-dimensional antiferromagnetic-ferromagnetic mixed spin- $1/2$ Lozenge chain at low temperatures were investigated using the transfer matrix method [50]. In the presence of crystal field interaction, some low-dimensional magnetic systems show magnetic plateaus [51] and it may affect some of the critical properties of the system. Beside the crystal field, some other examples for the mechanism of the magnetic plateaus in 1D spin chain can be given as dimerization, frustration and

* Corresponding author. Ecole Nationale Supérieure de Génie Énergétique et Procédés (ENSGEP) d'Abomey, Benin.

E-mail addresses: mounirou.karimou@yahoo.fr (M. Karimou), mehmet.bati@erdogan.edu.tr (M. Bati).

<https://doi.org/10.1016/j.ssc.2020.114137>

Received 13 July 2020; Received in revised form 4 September 2020; Accepted 5 November 2020

Available online 18 November 2020

0038-1098/© 2021 The Authors. Published by Elsevier Ltd. This is an open access article under the CC BY license (<http://creativecommons.org/licenses/by/4.0/>).

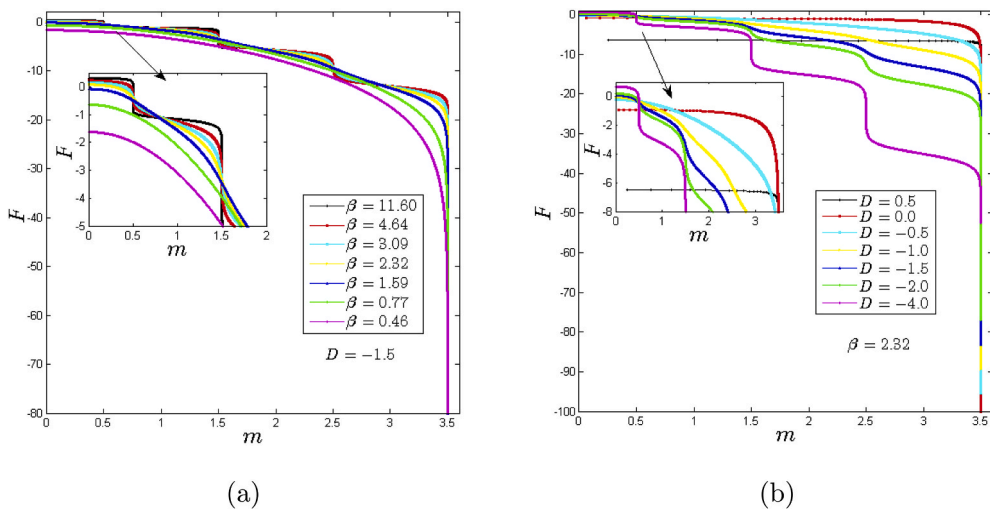


Fig. 1. (color online) Helmholtz free energy as a function of magnetization (a) for different reduced thermodynamic temperature at $D = -1.5$ (b) for different crystal field values at $\beta = 2.32$. (For interpretation of the references to color in this figure legend, the reader is referred to the Web version of this article.)

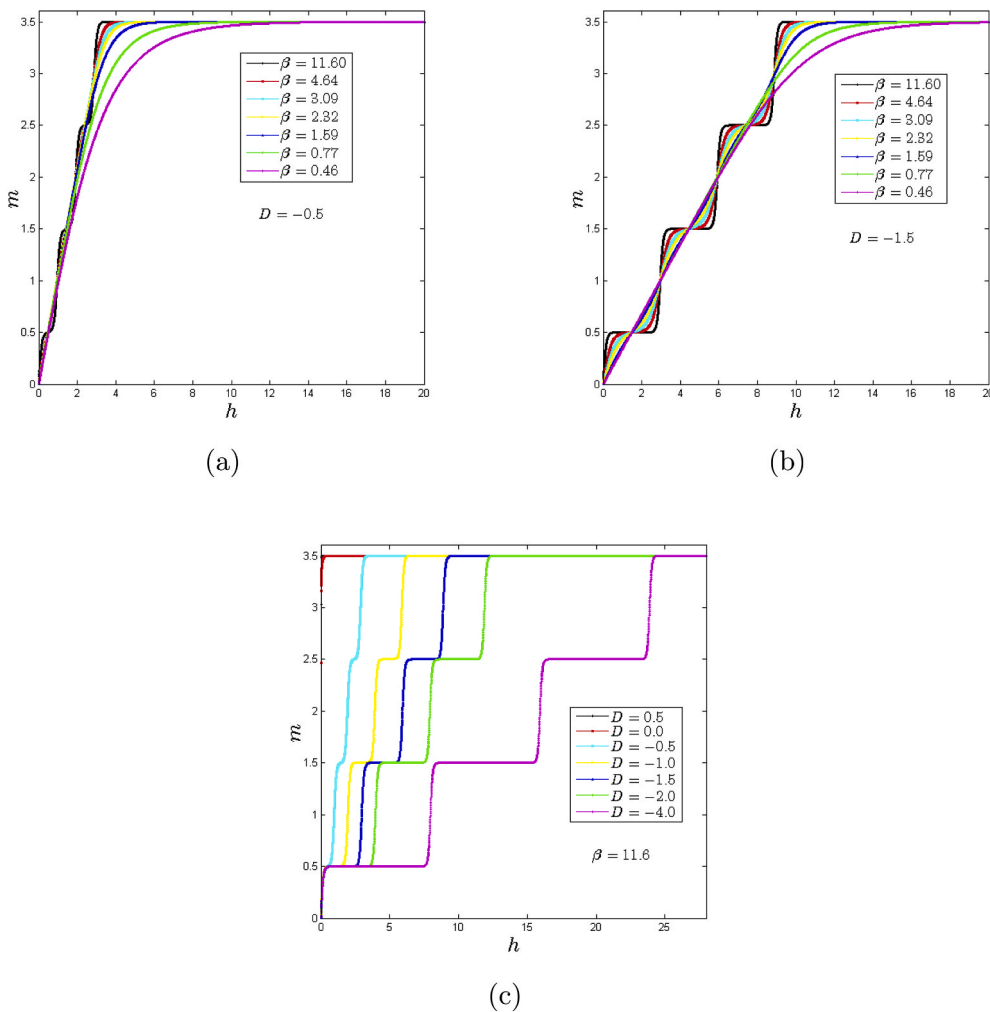


Fig. 2. (color online) Magnetization as a function of the reduced external magnetic field for selected values of the reduced thermodynamic temperature for (a) $D = -0.5$; (b) $D = -1.5$; and for selected values of the crystal field parameter for (c) $\beta = 11.6$. (For interpretation of the references to color in this figure legend, the reader is referred to the Web version of this article.)

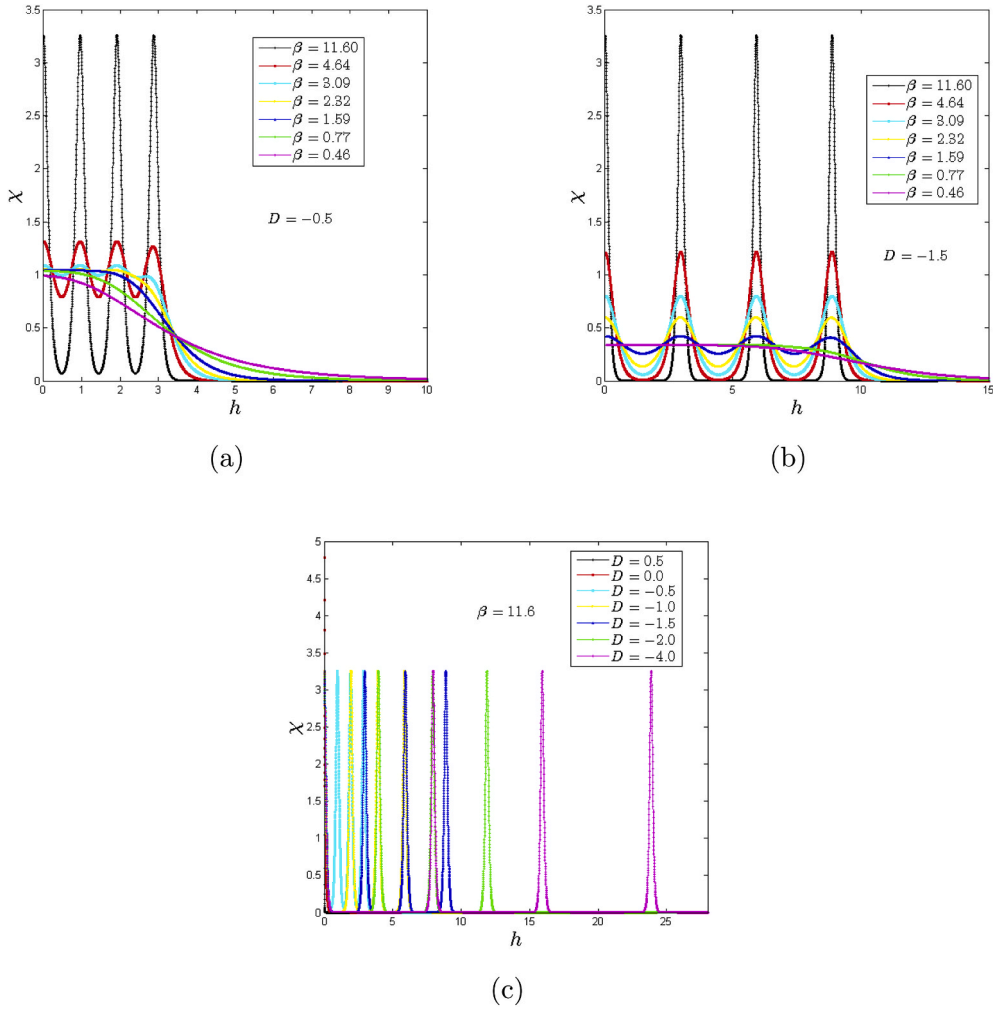


Fig. 3. (color online)Magnetic susceptibility as a function of the reduced external magnetic field for selected values of the reduced thermodynamic temperature for (a) $D = -0.5$; (b) $D = -1.5$; and for selected values of the crystal field parameter for (c) $\beta = 11.6$. (For interpretation of the references to color in this figure legend, the reader is referred to the Web version of this article.)

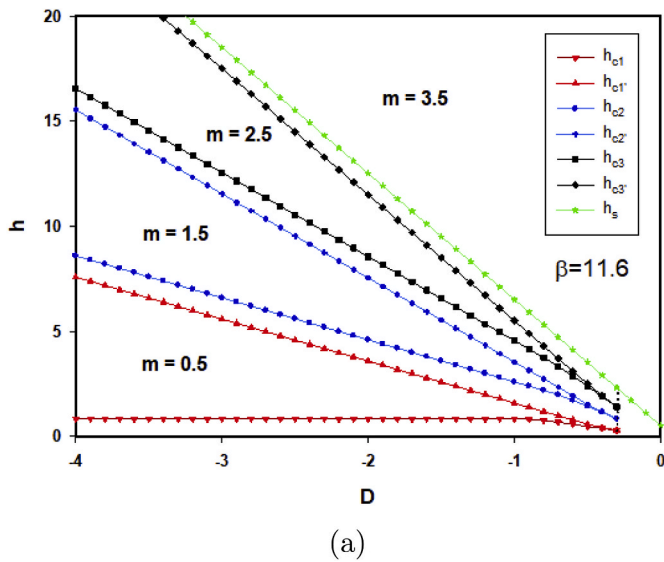


Fig. 4. (color online)The behavior of the plateau region transition depending on the crystal field at (a) $\beta = 11.6$ h_{ci} ($i = 1, 2, 3$) are critical field points for the positive magnetization values. (For interpretation of the references to color in this figure legend, the reader is referred to the Web version of this article.)

periodic field [52]. Sensoy and Bati [53,54] investigated the magnetic properties of spin-5/2 Ising chain by using TMM.

Thus, although a lot is known about the magnetic properties of the 1D chain consisting of low spins theoretically and experimentally, to our knowledge, for high spin values ($S = 7/2$) with crystal field interaction is not studied. In the present work, the magnetic properties of spin-7/2 BC chain under a magnetic field is addressed. We study the spin-7/2 in 1D chain system by using BC model with TMM. This model is a simple and successfully applied to investigate numerically the magnetic properties of the 1D systems.

The remaining part of the paper is organized as follows. In section 2, we present the model and formalism. The results and discussions are present in section 3. The present work is concluded in section 4.

2. Model and formulation

We will consider the following Hamiltonian to describe the system:

$$\mathcal{H} = -J \sum_i \sigma_i \sigma_{i+1} - \frac{D}{2} \sum_i (\sigma_i^2 + \sigma_{i+1}^2) - \frac{H}{2} \sum_i (\sigma_i + \sigma_{i+1}), \quad (1)$$

where each J denotes the exchange coupling of antiferromagnetic type ($J < 0$), D is the crystal field interaction parameters and H is in energy unit. J is used as an scaling factor through the work, and parameters are defined dimensionless form as reduced exchange coupling ($J = J/|J|$),

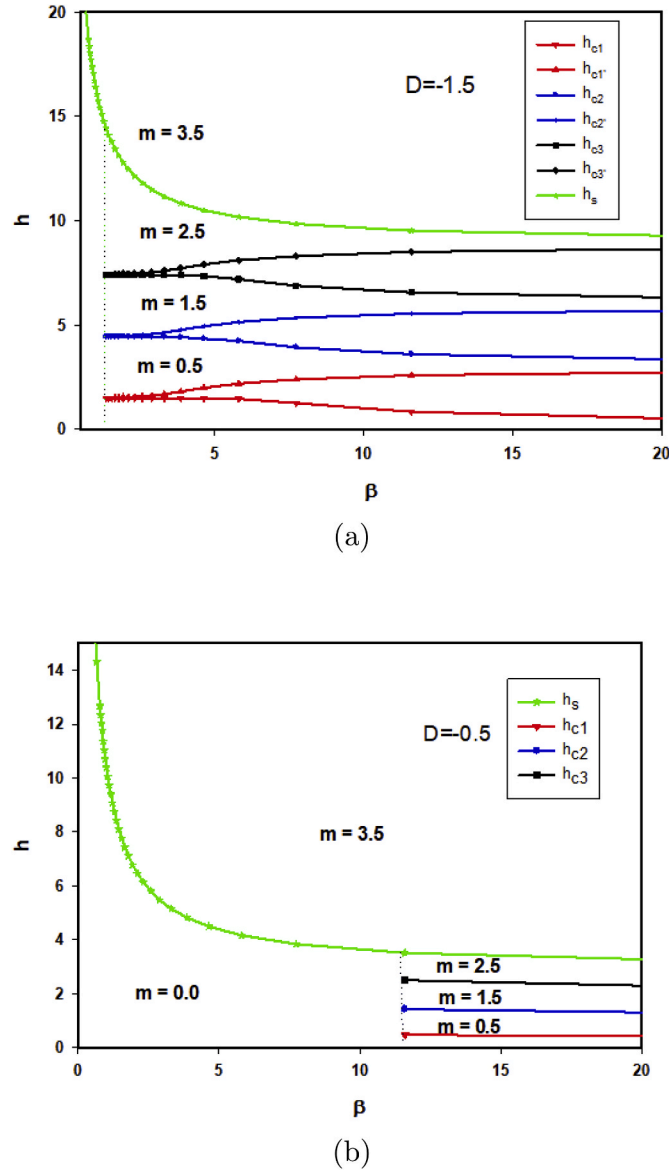


Fig. 5. (color online) The behavior of the plateau region transition depending on the reduced thermodynamic temperature at (a) $D = -1.5$; (b) $D = -0.5$. h_{ci} ($i = 1, 2, 3$) are critical field points for the positive magnetization values. (For interpretation of the references to color in this figure legend, the reader is referred to the Web version of this article.)

reduced crystal field ($D = D/|J|$) and reduced magnetic field ($h = H/|J|$). Using the **transfer matrix method formalism** [55,56], the **partition function (Z)** written as

$$Z = \sum_{\{\sigma_i\}} e^{-\beta \mathcal{H}(\{\sigma_i\})} = \sum_{\{\sigma_i\}} e^{\sum_i [\beta J(\sigma_i \sigma_{i+1}) + \frac{\beta D}{2}(\sigma_i^2 + \sigma_{i+1}^2) + \frac{\beta h}{2}(\sigma_i + \sigma_{i+1})]} \quad (2)$$

The elements of transfer matrix (TM) can be defined by

$$\langle \sigma_i | TM | \sigma_{i+1} \rangle = e^{\beta J(\sigma_i \sigma_{i+1}) + \frac{\beta D}{2}(\sigma_i^2 + \sigma_{i+1}^2) + \frac{\beta h}{2}(\sigma_i + \sigma_{i+1})} \quad (3)$$

The open form of the matrix is given in the appendix. Since the matrix is identical for $(\sigma_1 \sigma_2)$, $(\sigma_2 \sigma_3)$ and so on, the partition function Z is then given by

$$Z = \sum_{\{\sigma_i\}} (TM)^N = \text{Tr} \left[(TM)^N \right] = \sum_{i=1}^8 \lambda_i^N \quad (4)$$

where N is the number of spins in a one-dimensional lattice and λ is the eigenvalues of TM. The Helmholtz free energy can be written as

$$\begin{aligned} F &= -k_B T \ln \left(\sum_{i=1}^8 \lambda_i^N \right) \\ &= -k_B T \ln \left(\left(\lambda_1^N \left[1 + \left(\frac{\lambda_2}{\lambda_1} \right)^N + \left(\frac{\lambda_3}{\lambda_1} \right)^N + \dots + \left(\frac{\lambda_8}{\lambda_1} \right)^N \right] \right) \right) \end{aligned} \quad (5)$$

In the thermodynamic limit $N \rightarrow \infty$ only the larger one of the eigenvalues relevant because $\left(\frac{\lambda_i}{\lambda_1} \right)^N \rightarrow 0 (i = 2, 3, \dots, 8)$. Therefore the Helmholtz free energy per spin reads

$$F = -k_B T \ln(\lambda_1) \quad (6)$$

where λ_1 is the biggest eigenvalues of TM, k_B is the Boltzmann constant and T is the temperature. We have found the biggest eigenvalues of TM via the computer program and calculate the thermodynamic response function numerically. We evaluate the total magnetization per spin

$$m = - \left(\frac{\partial F}{\partial h} \right)_T, \quad (7)$$

the magnetic susceptibility

$$\chi = - \left(\frac{\partial^2 F}{\partial h^2} \right)_T, \quad (8)$$

The entropy

$$S = - \left(\frac{\partial F}{\partial T} \right)_h \quad (9)$$

and the specific heat

$$C = -T \left(\frac{\partial^2 F}{\partial T^2} \right)_h \quad (10)$$

where the derivatives are numerically obtained. The present formalism of TMM is entirely based on numerically exact calculations and allows for the calculation of magnetization properties for arbitrary finite temperatures and values of the Hamiltonian parameters.

3. Results and discussions

In this paper, we studied the magnetic properties of the anti-ferromagnetic spin 7/2 Blume-Capel chain system using the transfer matrix method. The average magnetization (m) was calculated with varying reduced crystal-field parameter (D) and reduced thermodynamic temperature $\beta = |J|/k_B T$ in the analysis of the magnetic behavior of the system.

We first look at the Helmholtz free energy of the system. The energy favors the largest possible value of m which is aligned with the applied field. Therefore, the equilibrium m value can be minimized by the Helmholtz free energy (F) (see Fig. 1). In Fig. 1 (a), we see that for different temperature values and the free energy is minimum at $m = 7/2, 5/2, 3/2, 1/2$. The antiferromagnetic system can either have $\pm 7/2, \pm 5/2, \pm 3/2, \pm 1/2$ values and thus, the F would choose only one favorite value for low temperature region but for higher temperature system only take spin $\pm 7/2$ values. **Similar results were found in the spin 5/2 system [53]. In this study, it was seen that the minimums occur at possible spin values.** In some materials, magnetization stays constant (a rational fraction of the saturated magnetization) for a finite range of magnetic field. This event is called the magnetization plateau. Plateau behavior is observed at high D values, whereas saturation magnetic field value is observed at low D values (see Fig. 1 (b)). We can say a gap mechanism appears if some kind of anisotropy is present in the system.

In Fig. 2, we have performed the magnetization behavior as a

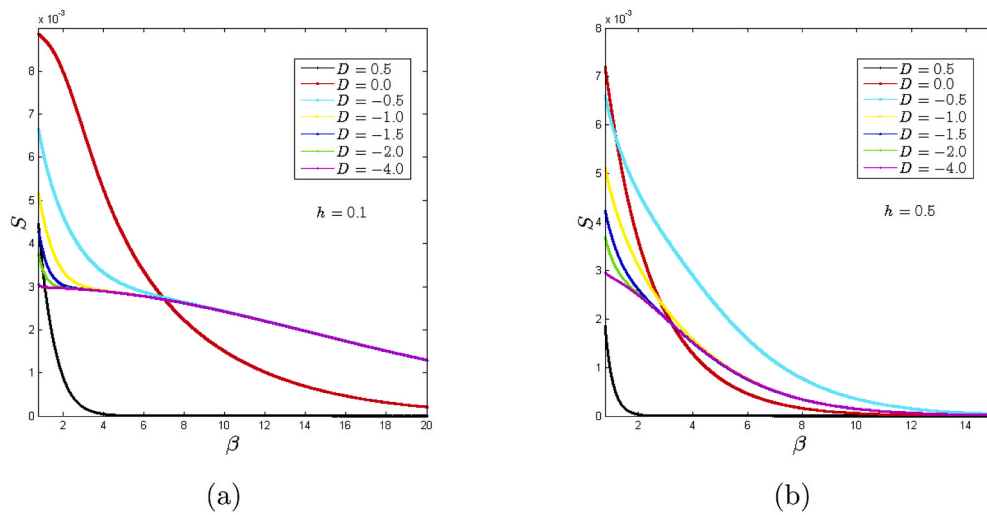


Fig. 6. (color online) Entropy as a function of the reduced thermodynamic temperature for (a) $h = 0.1$; (b) $h = 0.5$. (For interpretation of the references to color in this figure legend, the reader is referred to the Web version of this article.)

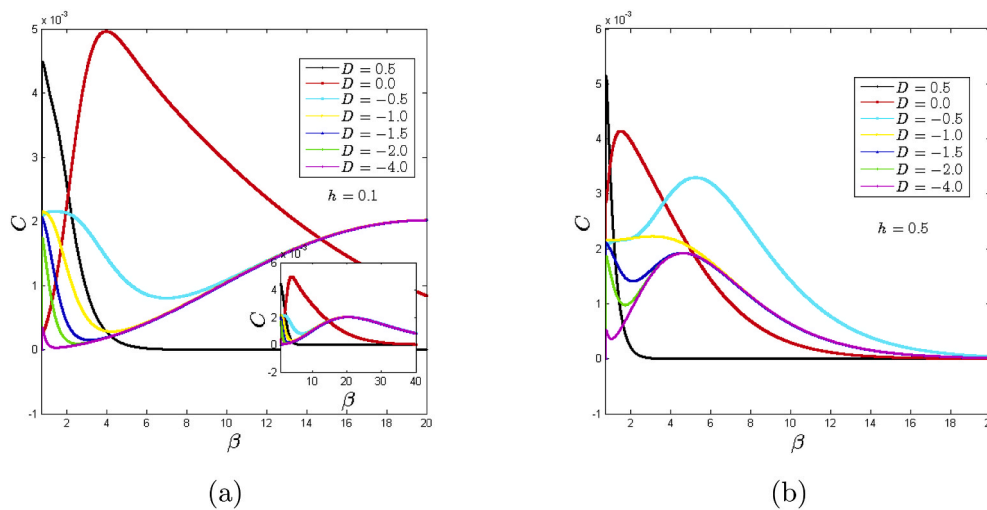


Fig. 7. (color online) Specific heat as a function as a function of the reduced thermodynamic temperature for (a) $h = 0.1$; (b) $h = 0.5$. (For interpretation of the references to color in this figure legend, the reader is referred to the Web version of this article.)

function of reduced magnetic field. The Magnetization as a function of the reduced external magnetic field for selected values of the reduced thermodynamic temperature Fig. 2 (a) for $D = -0.5$; Fig. 2 (b) for $D = -1.5$. The magnetization behavior for different D values at higher reduced thermodynamic temperatures ($\beta = 11.6$) are given in Fig. 2 (c). At low temperature (at high β) the spins align easily but contrary at high temperature to align the spins a strong magnetic field should be applied. We observed that the magnetization behavior with the change of magnetic field becomes more smooth and wider with the increase of the temperature. The magnetization becomes a step function at $\beta \rightarrow \infty$ ($T = 0$ K). Results show that the saturation at low temperature requires a small magnetic field, but at higher temperature values it requires higher magnetic field. For different reduced crystal field values as a function of the reduced external magnetic field h at $\beta = 11.6$. As expected, the saturation values of the magnetization are 3.5. We see from Fig. 2 (c) plateau region widened for higher crystal field values. **As a result we obtained the diagrams of magnetization processes for our system with the same magnetization plateau as in Ref. [51,57–65].**

Another way of the confirmation of multi plateau magnetization curves by numerical calculation in the Ising chain is to examine the magnetic field dependance of susceptibility (χ) as shown in Fig. 3. The

peaks in Fig. 3 indicate the critical fields for transitions from one plateau to another one. We also note that area between plateau regions correspond width of susceptibility peak. The susceptibility peaks show that the maximum for low temperature value. **In an experimental study by Shiramura and coworkers [57], the magnetization curve of a specific linear compound has plateaus and the peaks at critical field values were observed in magnetic susceptibility plots.**

In order to investigate the effect of single-ion anisotropy on the magnetization plateaus, the magnetization was calculated at finite h for different D values and the data were plotted as $D - h$ phase diagrams in Fig. 4.

For $D < 0.0$, four plateaus lines placed at $m = 0.5$, $m = 1.5$, $m = 2.5$ and $m = 3.5$ are divided by the critical field and saturated field lines as shown in Fig. 4 when $\beta = 11.6$. Furthermore, when $D > -0.2$ and positive D values only saturation values occur (Fig. 4). And out, in Fig. 4, in first critic field values (hc_1) magnetization become 0.5 and hc_1' magnetization become bigger than 0.5. In second critic field values (hc_2) magnetization become 1.5 and hc_2' magnetization become bigger than 1.5. In the third critic field values (hc_3) magnetization become 2.5 and hc_3' magnetization become bigger than 2.5. And finally in h_s magnetization saturated $m = 3.5$. Fig. 5 shows reduced thermodynamic

temperature versus magnetic field phase diagram plotted for (a) $D = -1.5$ (b) $D = -0.5$. We see from this Fig. 5 (a) plateaus region and transition area between plateaus region increase for increasing β (decreasing temperature). But for $D = -0.5$ in Fig. 5 (b) only saturation values occurs for low β values. We can see plateaus behavior only higher β values.

To show the influence of D on the entropy (S), we have illustrated in Fig. 6. The thermal variations of entropy for some values of the system parameters: $h = 0.1$ and $h = 0.5$ and varying D (see Fig. 6(a-b)). One observes that the entropy shows interesting behaviors. In Fig. 6 (a) for positive D values entropy goes to zero rapidly. In addition for all negative D values entropy of the system for $\beta > 8.0$ take almost the same values. But for higher h values entropy strongly depend on crystal field values (see Fig. 6 (b)). Moreover we see from these figures for $h = 0.5$ entropy goes to zero faster than $h = 0.1$ values. Entropy is a measure of the randomness or disorder of a system so if entropy goes to zero rapidly we see only saturation values of the system.

Finally, we have discussed another physical quantity which is the specific heat depends on the energy fluctuation of the system, for our model. We have calculated the reduced thermodynamic temperature behavior of specific heat at various D and h values, and the results are given in Fig. 7. The specific heat is a smooth function of temperature (finite at all temperatures). As expected there is no critical point at a finite temperature which corresponds to the singular behavior of specific heat. We can see in Fig. 7 (a) the specific heat shows a round maximum for $D = 0.0$. **Round maximum of the specific heat has been theoretically and experimentally detected in various systems [4,51,53, 54,61]**. For $D = 0.5$ $\beta \geq 4.75$ specific heat vanished. For negative D values the specific heat has a minimum at specific β values and has a maximum at $\beta = 20$ for all negative D values than decrease for increasing β values (please see inset of Fig. 7 (a)). We should note that the specific heat values are the same for negative D values at high β values. Fig. 7 (b) is plotted for different D values at $h = 0.5$. We see from this figure if the magnetic field is increased, the peak of the specific heat is shifted to lower β region and the specific heat vanished for high β values.

4. Conclusion

In this paper, the magnetic properties of the spin 7/2 Blume-Capel chain system have been studied by using a transfer-matrix method. Magnetic properties have been investigated at different reduced thermodynamic temperatures, the reduced crystal-field parameter and reduced magnetic field values. Thermodynamic response functions are obtained for varying values of reduced thermodynamic temperature and reduced magnetic field. We obtained the magnetization, susceptibility, entropy and specific heat. Our numerical results show that these thermodynamic response functions are strongly dependent crystal field parameters. We found that the system exhibits plateaus for negative crystal field values such as $D < -0.3$ for low temperature. **We also found that for the wider plateau, it is necessary to increase the crystal field values. Our results are conceptually consistent with the previous results for the lower spin chain systems [4,22,24,25]**. Finally, we hope that our study will provide a theoretical basis for researchers working on high-spin low-dimensional materials.

Declaration of competing interest

The authors declare that they have no known competing financial interests or personal relationships that could have appeared to influence the work reported in this paper.

Appendix

$$TM = \begin{pmatrix} \exp(-49a - 49b - 14c) & \exp(-35a - 37b - 12c) & \exp(-21a - 29b - 10c) & \exp(-7a - 25b - 8c) & \exp(7a - 25b - 6c) & \exp(21a - 29b - 4c) & \exp(\exp(35a - 37b - 2c)) \\ \exp(-35a - 37b - 12c) & \exp(-25a - 25b - 10c) & \exp(-15a - 17b - 8c) & \exp(-5a - 13b - 6c) & \exp(5a - 13b - 4c) & \exp(15a - 17b - 2c) & \exp(35a - 37b + 2c) \\ \exp(-21a - 29b - 10c) & \exp(-15a - 17b - 8c) & \exp(-9a - 9b - 6c) & \exp(-3a - 5b - 4c) & \exp(3a - 5b - 2c) & \exp(9a - 9b) & \exp(21a - 29b + 4c) \\ \exp(-7a - 25b - 8c) & \exp(-5a - 13b - 6c) & \exp(-3a - 5b - 4c) & \exp(-a - b - 2c) & \exp(a - b) & \exp(3a - 5b + 2c) & \exp(7a - 25b + 6c) \\ \exp(7a - 25b - 6c) & \exp(5a - 13b - 4c) & \exp(3a - 5b - 2c) & \exp(a - b) & \exp(-a - b + 2c) & \exp(-3a - 5b + 4c) & \exp(7a - 25b + 8c) \\ \exp(21a - 29b - 4c) & \exp(15a - 17b - 2c) & \exp(9a - 9b) & \exp(3a - 5b + 2c) & \exp(-3a - 5b + 4c) & \exp(-9a - 9b + 6c) & \exp(-7a - 25b + 10c) \\ \exp(35a - 37b - 2c) & \exp(25a - 25b) & \exp(15a - 17b + 2c) & \exp(37a - 25b + 6c) & \exp(3a - 5b + 4c) & \exp(-5a - 13b + 6c) & \exp(-21a - 29b + 10c) \\ \exp(49a - 49b) & \exp(35a - 37b + 2c) & \exp(21a - 29b + 4c) & \exp(37a - 25b + 6c) & \exp(-7a - 25b + 8c) & \exp(-21a - 29b + 10c) & \exp(-49a - 49b + 14c) \end{pmatrix}$$

where $a = \frac{\beta J}{4}$, $b = \frac{\beta D}{4}$, $c = \frac{\beta h}{4}$.

References

- [1] G.V. Kurlyandskaya, M.L. Sanchez, B. Hernando, V.M. Prida, P. Gorria, M. Tejedor, Appl. Phys. Lett. 82 (2003) 3053–3055.
- [2] C. Alexiou, A. Schmidt, R. Klein, P. Hüllin, C. Bergemann, W. Arnold, J. Magn. Magn Mater. 252 (2002) 363–366.
- [3] H. Zeng, J. Li, J.P. Liu, Z.L. Wang, S. Sun, Nature 420 (2002) 395.
- [4] E. Aydiner, C. Akyuz, Chin. Phys. Lett. 22 (2005) 2382.
- [5] F. Litaiff, J.R. de Sousa, N.S. Branco, Solid State Commun. 147 (2008) 494–497.
- [6] A.I. Proshkin, T. Yu Ponomareva, I.A. Menshikh, A.V. Zarubin, F.A. Kassan-Ogly, Phys. Met. Metallogr. 118 (2017) 929–934.
- [7] R.L. Bowden, D.M. Kaplan, J. Phys. 37 (1976) 803–811.
- [8] R. Baxter, Exactly Solved Models in Statistical Mechanics, Dover books on physics, Dover Publications, 2007.
- [9] Y. Liao, P.-X. Chen, Physica A 540 (2020) 123084.
- [10] T. Balcerzak, K. Szaowski, M. Jašćur, J. Magn. Magn Mater. 507 (2020) 166825.
- [11] A.V. Zarubin, F.A. Kassan-Ogly, A.I. Proshkin, J. Magn. Magn Mater. 514 (2020) 167144.
- [12] M. Suzuki, B. Tsujiyama S. Katsura, J. Math. Phys. 8 (1967) 124.
- [13] F.A. Kassan-ogly, Phase Transitions 74 (2001) 353.
- [14] P. Gambardella, A. Dallmeyer, K. Maiti, M.C. Malagoli, W. Eberhardt, K. Kern, C. Carbone, Nature 416 (2002) 301–304.
- [15] P. Gambardella, S. Rusponi, M. Veronese, S.S. Dhese, C. Grazioli, A. Dallmeyer, I. Cabria, et al., Science 300 (2003) 1130.
- [16] B. Gu, G. Su, Phys. Rev. B 75 (2007) 174437.
- [17] Y. Hosokoshi, K. Katoh, Y. Nakazawa, H. Nakano, K. Inoue, J. Am. Chem. Soc. 123 (2001) 7921.
- [18] R. Peka, D. Pinkowicz, Acta Phys. Pol., A 118 (2010) 959–961.
- [19] E.A. Harris, J. Owen, Phys. Rev. Lett. 11 (1963) 9.
- [20] D.S. Rodbell, J. Owen, J. Appl. Phys. 35 (1964) 1002.
- [21] K.S. Asha, K.M. Ranjith, A. Yogi, R. Nath, S. Mandal, Dalton Trans. 14 (2015) 44.
- [22] B. Sieklucka, D. Pinkowicz, Molecular Magnetic Materials: Concepts and Applications, John Wiley and Sons, 2017.
- [23] G.R. Wagner, S.A. Friedberg, Phys. Lett. 9 (1964) 11–13.
- [24] R. Dingle, M.E. Lines, S.L. Holt, Phys. Rev. 187 (1969) 643.
- [25] M.T. Hutchings, G. Shirane, R.J. Birgeneau, S.L. Holt, Phys. Rev. B 5 (1972) 1999.
- [26] J. Skalyo Jr., G. Shirane, S.A. Friedberg, H. Kobayashi, Phys. Rev. B 2 (1970) 4632.
- [27] W.J. Fitzgerald, D. Visser, K.R.A. Ziebeck, J. Phys. Chem. 15 (1982) 795.
- [28] K.W. Böer, U.W. Pohl, Magnetic Semiconductors in: Semiconductor Physics, Springer, Cham, 2014.
- [29] J. Strecka, M. Jascur, Acta Phys. Slovaca 65 (2015) 235–367.
- [30] R.K. Pathria, P.D. Beale, Statistical Mechanics, third ed., Academic Press, 2011.
- [31] D. Eloy, F. Ramos, J. Magn. Magn Mater. 323 (2011) 1934.
- [32] Y.D. Panov, J. Magn. Magn Mater. 514 (2020) 167224.
- [33] Z. He, Y. Ueda, M. Itoh, Solid State Commun. 141 (2007) 22.
- [34] J.A. Plascak, J.G. Moreira, F.C. Sá Barreto, Phys. Lett. A 173 (1993) 360.
- [35] H.K. Mohamad, Solid State Commun. 312 (2020) 113894.
- [36] H.K. Mohamad, H.A. Yasser, O.M. Nabeel, Solid State Commun. 308 (2020) 113832.
- [37] M. Keskin, O. Canko, B. Deviren, Phys. Rev. E 74 (2006), 011110.
- [38] O. Canko, B. Deviren, M. Keskin, J. Phys. Condens. Matter 18 (2006) 6635–6653.
- [39] M. Keskin, B. Deviren, O. Canko, M. Krak, Acta Phys. Pol. B 38 (2007) 2445–2457.
- [40] B. Deviren, M. Keskin, O. Canko, Comput. Phys. Commun. 178 (2008) 420–437.
- [41] O. Canko, B. Deviren, M. Keskin, Phys. Scripta 77 (2008), 055701.
- [42] B. Deviren, S. Akbudak, M. Keskin, Solid State Commun. 151 (2011) 193–198.
- [43] B. Deviren, M. Ertas, M. Keskin, Physica A 389 (2010) 2036–2047.
- [44] D.A. Garanin, H. Kachkachi, Phys. Rev. Lett. 90 (2003) 65504.
- [45] E. Albayrak, Physica A 390 (2011) 1529.
- [46] E. Albayrak, S. Akkaya, Phys. Scripta 76 (2007) 354–362.
- [47] E. Albayrak, S. Ylmaz, S. Akkaya, J. Magn. Magn Mater. 310 (2007) 98–106.
- [48] J.A. Plascak, P.H.L. Martins, Comput. Phys. Commun. 184 (2013) 259.
- [49] C.J. Silva, A.A. Caparica, J.A. Plascak, Phys. Rev. E 73 (2006), 036702.
- [50] H.H. Fu, K.L. Yao, Z.L. Liu, J. Magn. Magn Mater. 305 (2006) 253.
- [51] E. Aydiner, C. Akyüz, M. Gönülol, H. Polat, Phys. Status Solidi(b) 243 (2006) 2901.
- [52] X. Chen, Q. Jiang, W. Shen, C. Zhong, J. Magn. Magn Mater. 262 (2003) 258.
- [53] M.G. Sensoy, M. Bati, Physica E 113 (2019) 21.
- [54] M.G. Sensoy, M. Bati, Sakarya Univ. J. Sci. 22 (2018) 1901.
- [55] J. Yeomans, Statistical Mechanics of Phase Transitions, Oxford University Press, Oxford, UK, 1992.
- [56] K. Huang, Statistical Mechanics, second ed., Wiley, New York, 1987.
- [57] W. Shiramura, K. Takatsu, B. Kurniawan, H. Tanaka, H. Uekusa, Y. Ohashi, K. Takizawa, H. Mitamura, T. Goto, J. Phys. Soc. Jpn. 67 (1998) 1548–1551.
- [58] Y. Qi, A. Du, J. Magn. Magn Mater. 326 (2013) 171.
- [59] C. Ekiz, H. Yaraneri, J. Magn. Magn Mater. 318 (2007) 49–57.
- [60] G.-H. Liu, W. Li, W.-L. You, G. Su, G.-S. Tian, Solid State Commun. 166 (2013) 38–43.
- [61] X.Y. Chen, Q. Jiang, W.Z. Shen, C.G. Zhong, J. Magn. Magn Mater. 262 (2003) 258–263.
- [62] V.R. Ohanyan, N.S. Ananikian, Phys. Lett. A 307 (2003) 76–84.
- [63] D. Eloy, F. Ramos, J. Magn. Magn Mater. 323 (2011) 1934.
- [64] X. Chen, Q. Jiang, W. Shen, C. Zhong, J. Magn. Magn Mater. 262 (2003) 258.
- [65] M.A. Neto, J.R. de Sousa, N.S. Branco, Phys. Rev. E 91 (2015), 052153.